

New opportunities in science, materials, and biological systems in the low-gravity (magnetic levitation) environment (invited)

J. S. Brooks^{a)} and J. A. Reavis

Physics Department and NHMFL, Florida State University, Tallahassee, Florida 32310

R. A. Medwood

Atlantic High School, Delray Beach, Florida 33444

T. F. Stalcup

Physics Department and NHMFL, Florida State University, Tallahassee, Florida 32310

M. W. Meisel

Physics Department, University of Florida, Gainesville, Florida 32611

E. Steinberg, L. Arnowitz, and C. C. Stover

BioSpace International, Gaithersburg, Maryland 20877

J. A. A. J. Perenboom

Research Institute for Materials and High Field Magnet Laboratory, University of Nijmegen, Toernooiveld 1, NL-6525 ED Nijmegen, The Netherlands

We discuss new opportunities that present themselves with the advent of very high magnetic field resistive magnets with appreciable central bore access. A detailed description of the parameters of the magnetic force environment for the case of diamagnetic materials in a water-cooled Bitter-type resistive magnet is provided for the reader who may have an interest in low-gravity experiments. We discuss emerging research activities involving novel uses of magnetic forces in high field resistive magnets at the National High Magnetic Field Laboratory. Particular attention is given to the area of diamagnetic materials that allow a low or “zero” gravity state, i.e., magnetic levitation. These include studies involving plant growth, protein crystallization, and dynamics of single particles and granular materials. In the latter case, unique aspects of the magnetic force environment allow low gravity experiments on particulates that cannot be performed on the Space Shuttle due to the lack of a weak confining potential in space. © 2000 American Institute of Physics.

[S0021-8979(00)68308-1]

I. INTRODUCTION: DIAMAGNETISM

The main purpose of this paper is to bring to the scientific and technical communities an awareness of new opportunities that present themselves in the magnetic force environment of high field magnets, and to highlight the dc magnet facilities and activities at the National High Magnetic Field Laboratory.¹ The growing availability of high field resistive and superconducting magnets² has led to renewed activity^{3,4} and appreciation of diamagnetism (which is necessary for static magnetic levitation⁵). In light of these developments, there have been a number of very exciting magnetic force experiments recently, including popular articles and demonstrations,^{6–8} experiments on biological materials,^{9–14} and protein crystal growth.^{15–17} (We note however that applications of magnetic forces to biomolecules and polymers has been a well established area for quite some time.¹⁸) Very recently, it has been demonstrated that diamagnetic substances, including one’s fingertips, can be used in configurations that allow levitation of permanent magnets.¹⁹

Diamagnetism is induced in the atomic and molecular orbitals when a magnetic flux is applied to a material. A

simple classical argument²⁰ which treats an atomic orbital as a current loop in the presence of an applied field yields the approximate relation $\delta\mathbf{m} = -(e^2 r^2 / 4m)\mathbf{B}$. Hence the induced moment $\delta\mathbf{m}$ is diamagnetic, and is proportional to the average of the electron orbital radius r , and inversely proportional to the electron mass m . This relationship may be extended to consider enhanced diamagnetism in molecular or metallic systems where the orbits are larger, or where the effective masses are smaller.²¹ Graphite, antimony, and bismuth are such examples. Although the essential features of diamagnetism may be appreciated by classical arguments, the induced diamagnetic moment is in detail, a quantum effect,²² and $\delta\mathbf{m}$ does not dissipate as long as the external imposed magnetic field \mathbf{B} remains. Unlike the effects of eddy currents in metals, atomic and molecular diamagnetism produces a repulsive force in the presence of a *static* external magnetic field gradient. Many common materials are predominantly diamagnetic. In these cases the paramagnetic or ferromagnetic electron spins are absent, or their contributions to the overall susceptibility are very small. Hence only the diamagnetic contribution of the paired, core electron orbitals remain. An important example of a diamagnetic material is water, which is the main constituent in most living matter.

^{a)} Author to whom correspondence should be addressed; electronic mail: brooks@magnet.fsu.edu

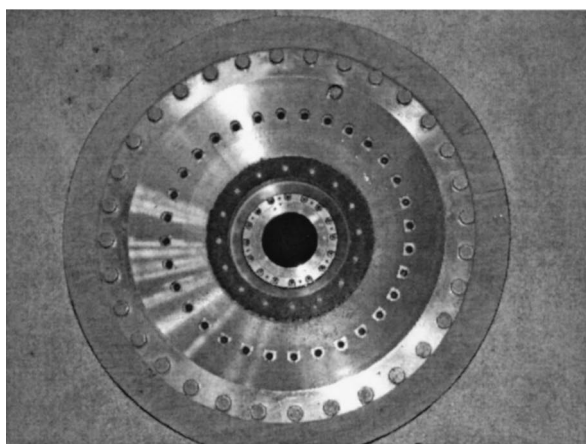
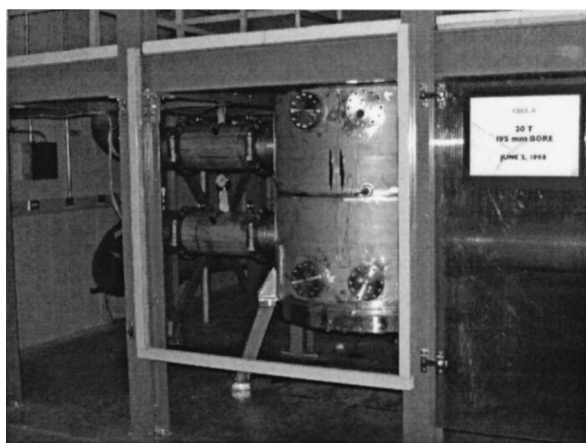


FIG. 1. Photograph of the 20 T, 195 mm bore resistive magnet at the NHMFL. (a) Side view. (b) Top view looking down on the 195 mm bore tube entrance (at center).

II. THE MAGNETIC FORCE (LOW-GRAVITY) ENVIRONMENT

In this paper we consider a high field resistive solenoid placed with its axis vertically (taken along z), parallel to the Earth's gravitational field. In Fig. 1 a 20 T, 195 mm bore resistive magnet at the National High Magnetic Field Laboratory (NHMFL) is shown. The center of the field is about 40 cm below the top of the bore tube. Experiments are inserted into the bore from above. The user has complete control of the magnetic field through a computer interface. At present 27 T, 50 mm and 33 T, 32 mm bore resistive magnets are also available to users, in a similar configuration.¹

In this section we take some care to describe the nature of diamagnetic materials in a high field resistive magnet, since it is not widely appreciated, even in the magnetism community. The main points to consider for experiments involving diamagnetic force experiments are listed below.

(1) For a given diamagnetic object, the balance equation in the simplest form is $(\rho/\chi)\mathbf{g}\mu_0 = \mathbf{B}d\mathbf{B}/dz$. This means that a diamagnetic object with density ρ and diamagnetic susceptibility χ will exhibit a magnetic force that opposes its gravitational weight for a particular value of the magnetic field-gradient product. Typical numbers for water ($\rho = 1000 \text{ kg/m}^3$, $\chi = 8.8 \times 10^{-5}/\text{m}^3$) give a field-gradient product of $BdB/dz = 1400 \text{ T}^2/\text{m}$. For graphite, on the other hand

TABLE I. Estimated variation of the diamagnetic force with sample radius for a 25 T, 50 mm bore resistive magnet, based on water in the levitated condition.

Sample radius	$\Delta g/g_0$
0.1 mm	10^{-6} (microgravity)
1.0 mm	10^{-3} (milligravity)
10 mm	10^{-1} (decigravity)

($\rho = 2280 \text{ kg/m}^3$, $\chi = 7.5 \times 10^{-5}/\text{m}^3$) the product is only $375 \text{ T}^2/\text{m}$. The point of balance will depend on the magnetic field \mathbf{B} and its axial gradient $d\mathbf{B}/dz$ —diamagnetic objects typically balance between 10 and 20 cm *above the center* of the magnet since a finite gradient is needed to produce a force.

(2) Because of radial gradients, diamagnetic objects are also repelled from the walls. This confines a levitated object. However, at a certain distance above the center of the magnet, the radial gradient reverses, and although objects may be forced upwards, they are also forced outwards against the bore tube. This can be seen by levitating an object and then increasing the field. (In Sec. IV exploitation of this effect for dynamics studies is described.)

(3) The combination of 1 and 2 in the presence of a gravitational field provide a stable equilibrium region where a diamagnetic object may “levitate.” This has the important effect that free objects are weakly confined, and can be studied without having to worry about collisions with boundaries. This is a distinct advantage over space shuttle experiments, where there is no weak confining potential.

(4) Due to anisotropy in shape and/or susceptibility, objects will align in specific directions with respect to the magnetic field direction.

(5) Microgravity is only reached for submillimeter size objects, due the fact that the field-gradient product is not constant. The deviation from microgravity with object size is shown in Table I. For large water droplets in the levitation condition, their shape becomes increasingly oblate with increasing diameter due to the vertical spatial inequality of the gravitational and magnetic forces.²³ We note that by specialized engineering, the product $\mathbf{B}d\mathbf{B}/dz$ can be made constant over a range of order 1 cm along the solenoid axis.²⁴

(6) Magnetic levitation is not the same physical effect as “zero gravity.” There are some fundamental differences in the mechanisms which lead to microgravity in a shuttle experiment and the $\mathbf{g}_{\text{eff}}=0$ condition in the field gradient environment. In earth orbit (the Shuttle), the effects are only gravitational and kinematic in origin; the earth's gravitational centripetal acceleration (GM/r^2) is balanced by the orbital centrifugal acceleration (v^2/r). This balance only involves consideration of the mass of the material, and Newton's Law ($\mathbf{F}=m\mathbf{a}$). At the atomic level, both the electrons and the nucleus have the same balance, since the mass of the orbiting material “drops out” of the balance equation, i.e., the condition depends only on velocity and orbit radius. One popular analogy is that the orbiting material is in continuous “free fall.” Magnetic levitation is distinguished from the above as follows: in diamagnetism, the magnetic force is primarily a result of the quantum electrodynamic action of

the magnetic field on the electrons. There is also an interaction on the nucleus (hence the phenomena of nuclear magnetic resonance and nuclear magnetism, etc.), but these nuclear forces are orders of magnitude smaller. Hence it is primarily the electrons that support the magnetic force in a material, and due to the very high stability of the atomic structure, the nuclei “follow along.” Again, the opposing gravitational acceleration acts on all masses in the atomic system.

(7) In multicomponent fluids, or where objects may be placed in fluids, or may crystallize from solution, one must consider *both* differentials in susceptibility and buoyancy in determining the effective acceleration.^{23,25}

(8) In the bores of room temperature access, water cooled resistive and helium cooled superconducting magnets, the temperature is generally less than room temperature, and may involve substantial spatial temperature gradients. The presence of air currents, and even strong air turbulence are clearly present in many cases.²⁶

III. SHUTTLE-TYPE EXPERIMENTS PERFORMED IN THE MAGNETIC FORCE ENVIRONMENT

The low-gravity environment offered in the high field resistive magnets can provide an important stepping stone for researchers who will perform, or who have already performed experiments on the Space Shuttle. Here we provide two such examples. The first involves the study of *Arabidopsis thaliana*, a rapidly maturing (4 weeks) mustard plant which is extensively studied by plant molecular geneticists.²⁷ This research, which involves determining which factors retard the growth of plants in zero gravity environments has already been carried out in the momentary milligravity environment of the NASA KC135 turbojet, and experiments have been flown on shuttle mission STS-93. The roots of the plants are genetically altered so as to contain a reporter gene that responds to stress.¹³ The stress may be measured after an experiment by observing the change in color (blue if stressed) of the roots when treated chemically. As an intermediate step, arabidopsis plants were placed simultaneously at the point of levitation (14 T, $BdB/dz = 1700 \text{ T}^2/\text{m}$), the magnet center (19 T, $BdB/dz = 0$), and in control experiments (0.1 mT or less) in the magnet cell. Their preliminary results¹³ show that there may be two effects which cause stress in the plants in the magnetic field environment: a background effect due to the magnetic field, and a low gravity effect (as already determined in the KC135 experiments). Further work presently underway by this group to understand more completely the effects of the magnetic levitation environment on living plants.

A second example is the work of BioSpace International²⁸ who have already performed two Shuttle flights where the crystallization of the bovine protein Ribonuclease S (Rnase S) has been carried out. Preliminary reports indicate that space-grown crystals of Rnase S show a systematic improvement of crystalline symmetry and apparent quality over earth-grown crystals, as determined by x-ray topography.²⁹ The goal is to see if the magnetic force environment can produce crystals of a comparable quality to space-grown crystals. (Clearly, earth-based crystallization

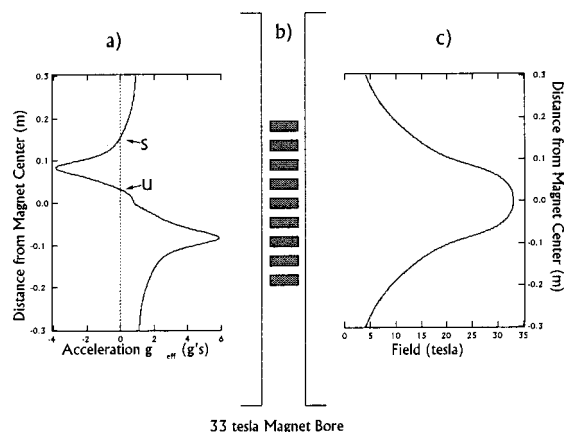


FIG. 2. Typical field and magnetic force parameters (for water) for a 33 T, 32 mm bore resistive magnet at the National High Magnetic Field Laboratory. For the case of maximum field (33 T), water-based samples can experience (as shown for different vertical displacements) an effective average body acceleration g_{eff} ranging from upwards, to zero, to downwards at six times the ambient gravitational acceleration. For *free body levitation* in this same magnet, objects such as oil, cork, and dense plastic levitate in the range 14.6, 15.6, and 16.96 T, respectively, at 8.7 cm above the magnet center.

carries a very substantial cost savings compared with a shuttle flight.) This group has taken a novel approach to the magnetic force environment, and is also taking temperature into careful consideration. A diagram of the BioSpace apparatus is shown in Fig. 2. For completeness, the example used is with a 33 T resistive magnet at the National High Magnetic Field Laboratory. In the BioSpace experiment, a novel consideration was made; not only can magnetic forces provide low gravity, they can also provide an enhanced acceleration (as in a centrifuge) by placing samples *below* the magnet center, and all effective g values in between. As shown in Fig. 2, if the magnet is run at full field, there is a distribution of effective gravity values ranging all the way from positive 6 g , through zero, to *negative* 6 g . In the BioSpace experiments the protein growth cells are arranged as shown along the axis of the magnet. Each cell has a growth chamber which is only a few mm^3 in volume, and the protein crystals in solution are significantly ($<100 \mu\text{m}$) smaller. Hence the radial forces may be minimized by placing the cells along the axis of the magnet (thereby minimizing the lateral forces of the growth chamber walls, and the vertical placement determines the effective g values). A second consideration is the temperature gradient that becomes an issue for vertically distributed growth cells involving biological materials. High field resistive magnets are water cooled, and the water, which is chilled, comes in at the top at about 10°C and exits at the bottom at about 40°C . (Because of the very high water pressure and the design of the plumbing, the acoustic vibration is minimal.) Since such temperature variations can greatly affect physical processes that involve biological materials, BioSpace has designed an insert where the temperature of each of the growth cells is controlled at 20°C individually. Preliminary protein crystal growth studies of Rnase S have recently been carried out by BioSpace in a zero g , 1 g , and 2 g configuration similar to that shown in Fig. 1. Here temperature regulation at 20°C was employed over a 3

$\frac{1}{2}$ day period where a high field resistive magnet was run continuously at 16 T. The results of the first experiment were a bit surprising, and show that in considering magnetic force experiments, the range of effective g values, both zero and greater than 1 g , is an important consideration. It was interesting to note that at zero g no crystals were formed. The results for the other 4 cells were as follows: at 0.5 g crystals of an undesirable shape formed; at 1 g and 1.5 g many 0.4 mm “normal” crystals formed, mostly against the wall of the growth chamber; at 1.5 g and at 2 g the “best” crystals; by visual inspection, of 0.6 mm in long dimension formed, but again against the growth chamber wall. At present, the x-ray topography is still in process, so the microscopic crystal quality is not yet known. Protein crystal growth, even under the most carefully controlled conditions, can be unpredictable, and further investigations are underway to determine the best conditions for crystallization in the presence of magnetic force.

It is clear that in the two experiments discussed above, there are many parameters to consider, especially in biological systems, in order to gauge the effects and benefits of the magnetic force environment. Nevertheless, systematic investigations to carefully sort out such details in a number of different biological and molecular systems is an emerging area of activity at the NHMFL. Other recent activities include alignment of carbon nanotubes, and magnetic force studies of blood, plants, and other biological materials.

IV. GRAPHITE COMPOSITES AND GRANULAR MATERIAL DYNAMICS

In Sec. II we described a unique set of experimental conditions which can provide a new dimension to research areas such as soft condensed matter physics. The examples given below exploit the capabilities of the 20 T, 195 mm bore resistive magnet at the NHMFL (see Fig. 1). This magnet has an advantage since the very wide bore allows excellent visual or instrumentation access to materials in the levitation region. (In the experiments described below, the data were taken by a video camera which was focussed on the magnet bore through a large mirror placed at the top of the magnet.) At present, the maximum field-gradient product is only 760 T²/m however, and water based materials, plastics, pure epoxy, etc. are not viable for levitation experiments. Graphite, however, with its very large, although highly anisotropic diamagnetic susceptibility,³⁰ can be easily levitated at about 16 T in this magnet. We have therefore exploited graphite-based epoxy composites to make objects for dynamic studies in the low gravity environment. Commercially available microcrystals of graphite, sold as a dry lubricant, align in the magnetic field such that the low susceptibility direction lies along the field. To avoid this, we have made graphite-epoxy composites (50%/50%), cured outside the field, to produce solid objects of various shapes with randomly oriented microcrystals. We first consider the center-of-mass motion of a small 1.2 g spherical rigid body. The three examples given below show the potential for future, more fundamental studies of particle dynamics and granular materials physics.

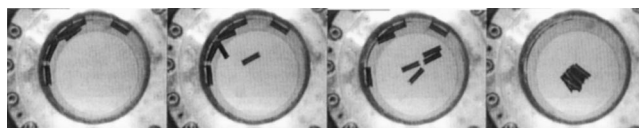


FIG. 3. Macroscopic crystal formation from rods (4 cm long). From left to right, the field is brought from 20 T to 16 T. The scale is set by the 195 mm bore tube diameter. The view is vertically downwards as videotaped through a mirror inclined at 45°.

A. Macroscopic crystallization

We show in Fig. 3 a sequence of frames where a set of nearly identical rods (~ 3 cm long and 1 cm in diameter) is placed at the bore tube wall at high field. (Here the high field/gradient product pushes the particle high enough to enter the region where the radial field gradient reverses sign.) The field is then lowered to a predetermined value where the rods levitate freely. The sequence shows that the kinetic energy of the rods, as they leave the wall, allow the assembly to find its most ordered state. By raising the field again the crystalline sample “melts,” and the process can be repeated again. It is possible to form the crystal by either changing the field very quickly (> 0.1 T/s) which is essentially a quenched condition, or very slowly. In such cases, disorder can be introduced into the final configuration.

B. Granular structures

In Fig. 4 we show a sequence of frames where a number of multicolored beads are brought in from the bore tube wall (by the method described in Sec. IV A) to form a “nucleus.” Since the beads are not identical, and have slightly different compositions and amounts of paint, they do not all sit in the same plane in the field, but have a vertical distribution. In the example shown, the field is reduced very slowly so that beads with a higher ρ/χ ratio enter the nucleus first, participate in the dynamics, and then exit the nucleus by dropping below. Particles which enter from the wall bring kinetic energy and angular momentum into the nucleus, and these effects can be seen dramatically in the nucleus dynamics for each collision. The nucleus does not have a surface tension, but is held together by the weak radial gradient forces. A point to make is that this sort of experiment cannot be done in the space shuttle, since there is no analogous restoring force. The macroscopic particle nucleus created in the magnetic force environment therefore presents a truly “new state” of a granular material.



FIG. 4. Macroscopic nucleus formation from beads (5 mm). The conditions are similar to those in Fig. 3. The object at magnet center is a U.S. dollar bill, which is paramagnetic and is attracted to the bore tube wall.

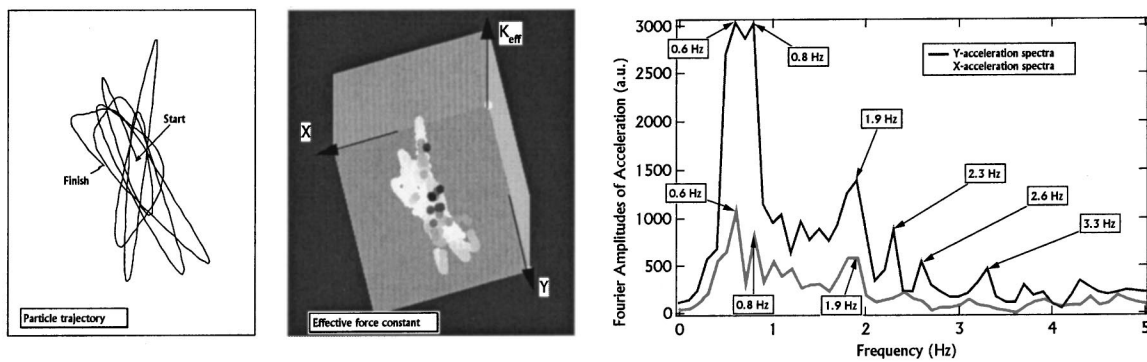


FIG. 5. Single particle dynamics of a 1.2 g spherical particle. The field is kept constant. The motion is only recorded for several seconds. (Full damping of the motion takes about 5 min.) (a) Spatial trajectory (dimensions comparable to 195 mm bore size in Figs. 3 and 4). (b) Surface plot of total effective spring constant (arbitrary units) vs spatial position. Reverse gray scale shows black dots in regions where k_{eff} is largest. (c) Fourier transform of acceleration components.

C. Single particle dynamics

In this experiment the initial state of the particle is prepared in a field well above the value needed for levitation, such that the particle is forced to the wall. The field is then lowered, either continuously, or in a single step, and the particle leaves the bore tube wall and begins a quasicyclic trajectory with a major period of order 1 s. Direct observation of the motion shows that the particle sometimes moves in a very nonharmonic manner, and sometimes even seems to reflect off of “invisible” spots in the magnet bore. To quantify this motion, we have digitized the trajectories $[x(t), y(t)]$ for numerical analysis. We then compute the velocity $[v_x(t), v_y(t)]$, the acceleration $[a_x(t), a_y(t)]$, and the instantaneous spring constant $[k_x = -ma_x/x, k_y = -ma_y/y]$. Finally, we compute the instantaneous vector sum $k_{\text{eff}} = (k_x^2 + k_y^2)^{1/2}$. In Fig. 5 we show the analysis from the digitized data, including the trajectory and a contour plot of the instantaneous spring constant vs the coordinates. Here we see that there are “high spots” in the magnetic force profile. This explains why the particle sometimes abruptly changes direction and velocity. Also shown are the Fourier components of the acceleration. Although the dominant frequency is similar to that observed by eye, there are other higher components which are not harmonics. In fact, the Fourier spectrum is different for the two orthogonal directions. We see, therefore that the motion not a simple harmonic oscillator.

The analysis above has assumed that the restoring forces are two dimensional and vertical motion has been ignored. We estimate that the vertical displacement is less than 1% of the in-plane motion. Also, there are several other forces that play a role, the damping due to the viscosity of air, and also convection currents, since no attempt has been made to block these currents. We note that by observing the particles for extended periods of time, the motion eventually damps out and we estimate that the wind currents are not a major input into the anharmonic behavior of the particles—rather, they arise from minor spatial variations in $\mathbf{BdB/dz}$.

D. Rigid body motion

Finally, we turn to an analysis of a rigid body. Here we have digitized the motion of two opposite points on an ir-

regular graphite block (“aquadag”). The center of mass motion and the angular acceleration is given in Fig. 5, where the spatial dependence of the instantaneous angular acceleration, which is directly related to the torque, is shown. By visual inspection, the object is observed to suddenly spin more rapidly as it executes its center of mass trajectory. Figure 5 shows that the major changes in the angular acceleration occur at certain points in the bore tube, where minor spatial variations in $\mathbf{BdB/dz}$ must be present. Due to the irregular shape of the block, a torque arises at these points (Fig. 6).

IV. CONCLUSIONS

The magnetic force environment of modern high field resistive magnets provide new opportunities for research in diverse areas. Such facilities have a place in the progress of selected space-based experimental programs. This is due to the cost differential of preparing experiments which involve low-gravity effects in earth-side laboratories prior to expensive shuttle flights. We have pointed out the differences between magnetic levitation and space environments, and note

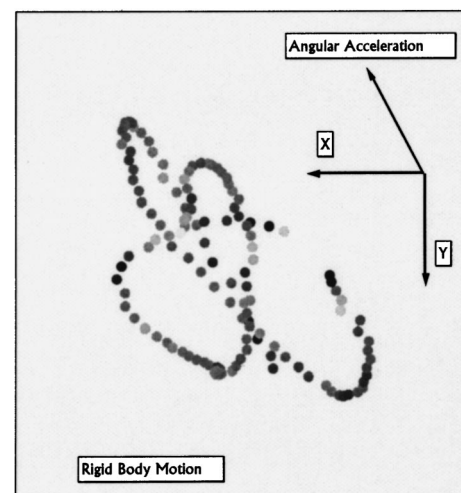


FIG. 6. Rotational dynamics of a rigid body. The angular acceleration (arbitrary units) for a rigid body vs center of mass position in the 195 mm bore magnet. The reversed gray scale shows places in the magnet where the angular acceleration is largest (black, counterclockwise; white, clockwise).

that the specific effects of magnetism and zero gravity on biological materials are in some sense largely unknown and controversial. Our point of view is that serious scientific studies are emerging in magnetic force experiments in high field resistive magnets due to their versatility, and that concrete results will be forthcoming in the next few years. And if true benefits can be had by processing or studying materials in high magnetic fields and gradients, then economical superconducting magnets can then be designed to accommodate specific applications for medical or industrial applications.

In the area of fundamental science, the “low-gravity laboratory” opens a new area of particle and many-body dynamics. To date, all earth-side experiments involving such systems (foams, beads, sand, etc.) have involved a confining surface, and in space-type experiments there is no confinement at all. In the simple examples above we have studied the dynamics of rigid bodies and their interactions in levitation configurations. We have learned, from the dynamics, details about the magnetic field/gradient product which clearly is not cylindrically symmetric in the case of the magnet shown. These simple studies lay the foundation for more interesting studies, including many-body effects and granular materials phenomena.

ACKNOWLEDGMENTS

The National High Magnetic Field Laboratory is supported by a contractual agreement between the National Science Foundation and the State of Florida. This work is sponsored in part by NHMFL/IHRP/NSF 500/5033.

- ¹B. Brandt, in <http://www.magnet.fsu.edu/user/facilities/dcfacilities/index.html>.
- ²H. J. Schneider-Muntau, *High Magnetic Fields: Applications, Generation, Materials* (World Scientific, Singapore, 1997).
- ³E. Beaugnon and R. Tournier, *Nature* (London) **349**, 470 (1991).
- ⁴E. Beaugnon and R. Tournier, *J. Phys. (France)* **III**, 1423 (1991).
- ⁵W. Z. Braunbeck, *Physics* **112**, 753 (1939).
- ⁶M. V. Berry and A. K. Geim, *Eur. J. Phys.* **18**, 307 (1997).
- ⁷A. K. Geim, *Phys. Today* **51**, 36 (1998).
- ⁸D. Schneider, *Am. Sc.* **87**, (1999).
- ⁹J. M. Valles *et al.*, *Biophys. J.* **73**, 1130 (1997).
- ¹⁰J. M. Denegre *et al.*, *Proc. Natl. Acad. Sci. USA* **95**, 147299 (1998).
- ¹¹J. M. Valles *et al.*, *Bull. Am. Phys. Soc.* **44**, 1720 (1999).
- ¹²H. Hirota, *J. Appl. Phys.* **85**, 5717 (1999).
- ¹³T. F. Stalcup *et al.*, in *Physical Phenomena in High Magnetic Fields III*, edited by Z. Fisk, L. Gor'kov, and R. Schrieffer (World Scientific, Singapore, 1999) p. 659.
- ¹⁴M. W. Meisel *et al.*, *Bull. Am. Phys. Soc.* **44**, 1720 (1999).
- ¹⁵N. I. Wakayama *et al.*, in *Physical Properties in High Magnetic Fields*, edited by Z. Fisk, L. Gor'kov, and R. Schrieffer (World Scientific, Singapore, 1999), p. 598.
- ¹⁶N. I. Wakayama, M. Ataka, and H. Abe, *J. Cryst. Growth* **178**, 653 (1997).
- ¹⁷M. Sato, *J. Phys. C* **17**, L817 (1984).
- ¹⁸G. Maret and K. Dransfeld, in *Strong and Ultrastrong Magnetic Fields and Their Applications*, edited by F. Herlach (Springer-Verlag, Berlin, 1985), Vol. 57, p. 143.
- ¹⁹A. K. Geim *et al.*, *Nature* (London) **200**, 323 (1999).
- ²⁰D. J. Griffiths, *Introduction to Electrodynamics* (Prentice-Hall, Upper Saddle River, 1989).
- ²¹E. W. Lee, *Magnetism: An Introductory Survey* (Dover, New York, 1970).
- ²²J. H. v. Vleck, *The Theory of Electric and Magnetic Susceptibilities* (Oxford University Press, London, 1965).
- ²³Y. Ikezoe *et al.*, *Nature* (London) **393**, 749 (1998).
- ²⁴M. Bird (private communication).
- ²⁵N. I. Wakayama, *J. Appl. Phys.* **81**, 2980 (1997).
- ²⁶A. K. Geim, *Phys. Today* **51**, 11 (1998).
- ²⁷D. W. Meinke *et al.*, *Science* **282**, 662 (1998).
- ²⁸E. S. L. Arnowitz, BioSpace International, Gaithersburg, MD 20877.
- ²⁹T. Gallagher *et al.* (to be published).
- ³⁰M. P. Sharma, L. G. Johnson, and J. W. McClure, *Phys. Rev. B* **9**, 2467 (1974).